Multi-User Beamforming and Transmission Based on Intelligent Reflecting Surface

Yihong Liu, *Graduate Student Member, IEEE*, Lei Zhang, *Senior Member, IEEE*, and Muhammad Ali Imran, *Senior Member, IEEE*

***Abstract*— Intelligent Reflecting Surfaces (IRS) show a revolutionary potential for wireless communications. In this paper, a single IRS is used to achieve distributed multi-user beamforming and interference-free transmission. We first establish the IRS assisted multi-user system model and formulate an optimization problem called multi-user linearly constrained minimum variance (MU-LCMV) beamformer, under the criterion of minimizing the overall received signal power subject to a certain level of power response (e.g., unit power response) at desired signal directions and arbitrary low power response (e.g., zero power response) at the interference directions. A closed-form amplitude-unconstrained phase-continuous (AUPC) solution is derived first, then an amplitude-constrained phase-continuous (ACPC) solution is obtained by using sequential quadratic programming (SQP). Given the solutions, the IRS beam pattern shows that to achieve multi-user (N pairs of transceivers, $N > 1$) transmission through a single surface, up to $N - 1$ redundant beams are generated, significantly affecting power efficiency. The directions of the redundant beams are mathematically derived. The effect of mutual coupling on IRS is also analyzed to show the characteristic of side lobes. Simulation results verify the existence and accuracy of the redundant beam directions. This work can potentially enhance state-of-the-art wireless communication systems ranging from transceiver design, system and architecture design, network deployment and self-organizing-network operations.**

***Index Terms*— Intelligent reflecting surface, beamforming, redundant beam, MIMO.**

I. Introduction

THROUGH the generations of wireless communication evolution, spectrum efficiency and power efficiency are two of the most important metrics to measure the system performance. Tremendous endeavors have been devoted to enhancing them through the system, architecture, algorithm and protocol, and hardware design. There are many factors that can fundamentally limit the wireless communication system performance while the wireless channel is of the most critical, intractable, but indispensable ones since it is uncontrollable and unpredictable. The signal carried by electromagnetic (EM) wave travels through the environment may suffer from many channel effects such as path-loss, fading, shadowing, etc. Spectrum and power efficiency of the wireless communication system are determined by the channel and the means of how to combat it. Path-loss is typically determined by the propagation environment, propagation medium and the distance between the transmitter and the receiver. To compensate path-loss, transmission power and/or receiver sensitivity can be increased at the cost of reducing power efficiency and/or increasing the system complexity. Multi-antenna beamforming and relay techniques are other typical approaches to compensate for the signal power loss over the channel, at the cost of extra required space, power, and complexity. The path-loss for high-frequency bands, such as millimeter wave, is even worse and has to be compensated by large scale antenna array (or directional antenna) at the transceivers [2].

Multi-path effect produces channel fading and inter-symbol interference (ISI) which is detrimental to the communication quality. To overcome this effect, elaborate techniques have been proposed across all modules in the baseband procedures, e.g., multi-carrier systems such as orthogonal frequency-division multiplexing (OFDM) [3], advanced channel estimation and equalization algorithms [4], [5], adaptive modulation and coding schemes [6], [7], and various detection algorithms [8], [9]. Nevertheless, the complexity of signal processing algorithm, protocol, and system within the transceiver is extremely high and thus brings significant cost.

Thanks to the multiple-input-and-multiple-output (MIMO) technique and other advanced multi-antenna approaches such as massive MIMO [10]–[12] and millimeter-wave (mmWave) communications [2], faster communication and better spectrum utilization can be achieved. Theoretically, the MIMO system has the ability to scale the capacity of a wireless connection by introducing multiplexing gain and/or diversity gain. However, the realistic scalability of MIMO system may be seriously limited due to the cost of RF chains, and the uncontrollability plus randomness of the wireless channel [13], [14]. As a result, considerably overhead and resources are required for channel estimation and equalization. Additionally, the rank of the channel matrix of a MIMO system is fully determined by the communication environment. Thus, the multiplexing gain is limited by the channel even with full channel knowledge. On the other hand, enforcing

Manuscript received 17 June 2021; revised 9 January 2022; accepted 2 March 2022. Date of publication 15 March 2022; date of current version 12 September 2022. This work was supported in part by the U.K. Engineering and Physical Sciences Research Council (EPSRC) under Project EP/V519686/1 and Project EP/S02476X/1. An earlier version of this paper was presented in part at the IEEE Global Communications Conference (GLOBECOM) 2019 [DOI: 10.1109/GLOBECOM38437.2019.9013433]. The associate editor coordinating the review of this article and approving it for publication was V. Sciancalepore. *(Corresponding author: Lei Zhang.)*

The authors are with the School of Engineering, University of Glasgow, Glasgow G12 8QQ, U.K. (e-mail: y.liu.6@research.gla.ac.uk; lei.zhang@glasgow.ac.uk; muhammad.imran@glasgow.ac.uk).

Color versions of one or more figures in this article are available at https://doi.org/10.1109/TWC.2022.3157808.

Digital Object Identifier 10.1109/TWC.2022.3157808

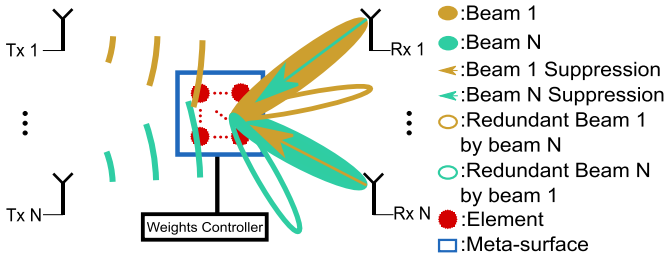

Fig. 1. MU beamforming and transmission based on IRS (Peaks and zeros can be formed for desired signal and interference respectively. Redundant beams will be generated for optimal beamforming to support multi-user transmission by a single IRS).

orthogonality among the data streams causes a power loss, and thus a beamforming gain limitation (i.e., decomposition reduces the strength of eigenvalues in the eigenvectors). It would be no doubt that how significant revolution of wireless communication can achieve if we can control the channel. The recent advance on EM materials found possibility from a new type of retrofitted low-cost material [15], usually called meta-material [16]. The artificial thin film of this material is usually referred to as reconfigurable intelligent surface (RIS) [17], intelligent reflecting surface (IRS) [18], or meta-surface [19]. An IRS can be a very simple structure, comprising a set of conductive patches, diodes, and conductive power/signal lines. By integrating artificially designed electronic elements, i.e., PIN diode, in the surface of meta-material, IRS is shaped [20]. Meanwhile, the excitation and phase of each electronic element can be controlled by processors (e.g., Field Programmable Gate Array FPGA) [15], [21], thus the phase and amplitude of the EM wave impinging on the surface can be manipulated and reflected to any desired directions. Therefore, the wireless channels within the natural environment become controllable with such surface posting on the basic building block (e.g., can even replace the traditional surface of the ceiling and wall) [22]. In addition, due to its ability to manipulate the EM wave and the communication channel, it is expected to be a driving technology of 6G and leading a disruptive evolution [23]. From those perspectives mentioned above, it is the first time for us to be able to (at least partially) control/program the wireless channel by which the customized wireless communication environments can be achieved. In other words, those objects, e.g., buildings or indoor walls which bring negative effects to the signal transmission, can turn into something helpful to produce more design degrees of optimization with the coating of such IRS on those objects [19]. It is worth noting that the IRS, from the architecture perspective, as shown in Fig. 1, is similar to a multiple antenna relay system [24]. However, the principles, challenges, and applications of them are different. The IRS *reflects* impinging signals (at some specific frequency bands) as an object rather than *re-transmit* the received signal as a transmitter in the relay systems. From this point of view, it is an EM mirror that can reflect the signal to *arbitrary* direction by controlling the phase/amplitude of the elements on the surface. Unlike the *active* relay system relies on multiple radio frequency (RF) chains, the IRS is *passive* so that it can be made as thin as a wallpaper to be posted on any physical surfaces and therefore it is low cost, low power, flexible, and scalable [22]. Besides, the *active* relay system typically works in a half-duplex manner to avoid interference while IRS has no such constraint (i.e., it can achieve full-duplex function without generating interference) [19], [25]. As such, passive surfaces are different from active antenna arrays.

Extensive research has been done for IRS in beamforming, channel estimation, resource allocation and implementation, etc. [20]–[22], [26]–[31]. Some work presented multi-input-single-output (MISO) model of IRS using gradient-based energy efficiency maximization algorithm and deep learning algorithm to design phase control [17], [31]. MIMO model of IRS also have been proposed and analyzed by using well-known minimal mean-squared error (MMSE) and zero forcing (ZF) beamforming [18]. In addition to that, some work focused on the IRS based channel estimation [28], [29] and resource allocations [32]. Also the experimental realization is given in different applications [21], [27]. Most of the aforementioned works apply IRS into low frequency band and assume the fading channel between transmitter and IRS, and from IRS to the receiver. However, to the best of the authors' knowledge, IRS used in high frequency band is less focused. In fact, IRS can be more useful in mmWave and Terahertz (THz) communications due to their severe coverage issues. Thus, a complete channel/system model and optimization formulations are required. Moreover, a well considered and thorough analysis on realizing multi-user transmission through a single IRS in such a system is unknown. With the revolutionary idea, it is also worth to investigate the physical properties and constraints of IRS to provide some insights and guidance for the IRS assisted wireless communication system design.

In this paper, our study focuses on IRS based multi-user beamforming and transmission. Such a scenario can also be viewed as a special form of single-user MIMO. We first formulate a cost function by minimizing total received power at users while satisfying conditions for securing effective communication and suppressing interference. A novel multi-user linearly constrained minimum variance (MU-LCMV) is proposed to obtain the optimal solution for nullifying the known interference and minimizing the unknown interference. For example, in the case of two pairs of transceivers, the signal transmitted from `Tx1` to `Rx1` through the reflection of IRS is kept above a certain response level while that of reflected towards to `Rx2` is nullified and any interference from unknown directions can also be minimized. Vice versa for the signal transmitted from `Tx2` to `Rx2`. This can be implemented through designing the beamforming weights for the elements on the IRS and controlled through the weights controller [33], [34], as shown in Fig. 1. Due to the particular working principle with solutions in IRS [33], [34], we observed that redundant beams[1] are formulated in addition to the main desired beams. The existence of redundant beams

[1]It could be found that by realizing multi-user transmission on a single surface, not only the main beams will be steered to desired directions, there might be redundant beams pointing to other directions. This phenomenon will be discussed in Section IV.

are proved and systematically analyzed in various cases. This unique property in IRS may significantly affect power efficiency and generate extra interference at unwanted directions. To summarize, the main contribution of this paper is as follows.

- We first propose the IRS assisted multi-user channel model based on a *single* piece of IRS, which can support multi streams transmission. Additionally, fundamental limitations on directions of the transceiver are derived for practical deployment. Based on the proposed model, IRS assisted multi-user optimization problems are formulated. A closed-form amplitude-unconstrained phase-continuous (AUPC) solution is derived first, and then practical amplitude-constrained phase-continuous (ACPC) solutions are achieved by using sequential quadratic programming (SQP) method and regularized MU-LCMV beamformer.
- Secondly, the insights of the redundant beam has been exploited and discussed theoretically while considering the general URA scenario. This conclusion can provide a guideline for further designs on IRS' deployment and resource management due to the redundant beams essentially split the energy. Therefore, relative considerations are required to avoid it or leverage it to support multi-cast communication in some specific scenarios.
- Lastly, after comparing with the existing algorithms, our proposed SQP algorithm outperforms others on the solvability since it is able to search the infeasible points without caring the feasibility of constraint, which always can return a solution given the restricted nonlinear conditions. In addition, we propose two MU-LCMV based solutions that are in low-complexity, and they can be used in some real applications to give a satisfied performance.

The rest of the paper is organized as follows. In Section II, we build an IRS system model. In Section III, the optimization problem of multi-user based on IRS is formulated and three solutions to the optimization problem are derived. In Section IV, we give the corollaries of redundant beams for both commonly used uniform linear array (ULA) and uniform rectangular array (URA) as examples. Simulations and conclusions are given in Section V and Section VI, respectively. Proofs of corollaries are given in Appendix A.

Throughout this paper, bold-faced upper case letters, bold-faced lower case letters, and light-faced lower case letters are used to denote matrices, column vectors, and scalar quantities, respectively. $E\{\cdot\}$ is the expectation operator and $\triangleq$ represents equivalent in terms of the optimization. The superscripts $(\cdot)^T$ and $(\cdot)^H$ represent matrix (vector) transpose, complex conjugate transpose, respectively. $\odot$ denotes pointwise multiplication. $\mathbf{I}$ is the identity matrix.

II. System Model

In this section, we model a distributed multi-user system based on a common single IRS, which takes the role of steering the multiple beams to the desired directions while suppressing the interference from unwanted directions. The considered system contains N pairs of transceivers where each transmitter and receiver is equipped with a single antenna. The IRS is composed of M elements, and in theory, the shape of the IRS and the geometry configurations of these elements on the surface can be arbitrary, since all space distributed elements can be represented in the form of steering vector with specific delay in directions of interest.

The channel model of IRS considered in this paper is NLOS, which is a long-lasting issue in mmWave communications [35]–[37]. Then, there are several assumptions. Firstly, line of sight (LOS) paths are considered between the Tx to IRS and IRS to Rx and there is no direct link between Tx and Rx. This assumption can be justified since IRS can play more important roles in the case of no LOS path exists between Tx and Rx. This can be very common and an imperative issue in high-frequency band (e.g., mmWave) communications. Next, for the channel fading and path-loss, usually quasi-static flat fading or block fading is considered [18], [28]–[31]. Since we analyze a single frame narrowband signal, an ideal case of far-field transmission with no channel path-loss and fading is considered. But our conclusions can be extended into the more generic channel with path-loss and fading straightforwardly. Lastly, global channel state information (CSI) availability at IRS is assumed in this paper and it is a common assumption in lots of works [17], [18], [30], [31], [38]–[41]. Actually, acquiring CSI requires sophisticated channel estimation by sending training pilot through direct BS-user link and BS-IRS-user link [42]. During channel estimation, the on-off statement and phase shifts of elements are jointly controlled in a predefined way by BS along with the training pilot sent by transmitters [28], [39]–[41]. Once channel is estimated, it would be sent to IRS via the internet link between BS-IRS for beamforming [38].

A. IRS Multi-User Model

Considering an IRS with M elements that is deployed for N pairs of single antenna users communication, the signal impinges on the IRS can be expressed as

$$\mathbf{y}_s = \mathbf{A_{in}}\mathbf{s}, \tag{1}$$

where $\mathbf{s} = [s_1, s_2, \ldots, s_N]^T \in \mathbb{C}^{N\times 1}$ is the source signal vector and s_i $(i = 1, 2, \cdots, N)$ is the signal for the i-th pair of transceiver. $\mathbf{A_{in}}$ is the channel matrix from the transmitters to the IRS, which can be represented by the matrix composed of steering vectors as

$$\mathbf{A_{in}} = [\mathbf{a}(\Omega_{in,1}), \mathbf{a}(\Omega_{in,2}), \ldots, \mathbf{a}(\Omega_{in,N})] \in \mathbb{C}^{M\times N}, \tag{2}$$

where $\mathbf{a}(\Omega_{in,i})$ is i-th user's steering vector of incident directions and $\Omega_{in,i}$ is the term containing the spatial information of incident directions from i-th transmitter $\mathtt{Tx}_i$. According to the antenna array theorem, Ω is a function of azimuth and elevation angles for two-dimensional deployment (e.g. URA), or only contains only one-dimensional information of azimuth angle such as ULA. Note that there is no noise in equation (1) since the IRS is a passive system, which is different from relay systems. Though this model is suitable for all frequency

bands, however, it is particularly useful for mmWave communications, which suffer from severe coverage issues.

On the IRS, each element will reflect the impinging signal from the Tx. However, by controlling the phases at the elements, the phase of the reflected signal at each element can be different. Optimal weights can be calculated to assure that the signals are coherently added at the direction of Rx. As one of the implementations, the elements' phases can be controlled by a biasing circuit switch (e.g., as proposed in [20]). Thus, the weighted signal at the surface can be written as

$$\hat{\mathbf{y}}_s = \mathbf{W}\mathbf{y} = \mathbf{W}\mathbf{A}_{\mathbf{in}}\mathbf{s}, \tag{3}$$

where $\hat{\mathbf{y}}_s$ is the phased signal on IRS, the weights matrix $\mathbf{W} \in \mathbb{C}^{M\times M}$ is a diagonal matrix with each entity on the diagonal being the weight of each element.

At the receivers, the received signals reflected from the IRS are phased by another matrix of steering vectors $\mathbf{A}_{\mathbf{out}}$ which defined as

$$\mathbf{A}_{\mathbf{out}} = [\mathbf{a}(\Omega_{out,1}), \mathbf{a}(\Omega_{out,2}), \ldots, \mathbf{a}(\Omega_{out,N})] \in \mathbb{C}^{M\times N}. \tag{4}$$

The $\mathbf{A}_{\mathbf{out}}$ has the same form as $\mathbf{A}_{in}$ in (2). $\Omega_{out,i}$ contains direction of i-th receiver Rx_i. $\mathbf{a}(\Omega_{out,i})$ represents the steering vector of exit angles of phased signals from the IRS to Rx_i. Thus, the received signal $\hat{\mathbf{y}}_r$ at all N receivers can be expressed as a vector form

$$\hat{\mathbf{y}}_r = \mathbf{A}_{out}^T \mathbf{W}\mathbf{A}_{in}\mathbf{s} + \mathbf{n}, \tag{5}$$

where the $\mathbf{n}$ is the noise vector at the receivers. The weights matrix, $\mathbf{W}$ needs be solved and applied on the surface to make sure the reflected signals are optimally reflected towards the desired direction without cross-interference among the users. As the incident steering vectors and exit steering vectors respect to the IRS are independent to each other and both controlled by the weights at same time, to this end, we merge $\mathbf{a}(\Omega_{in,u})$ and $\mathbf{a}(\Omega_{out,v})$ as a compound steering vector

$$\mathbf{a}_C(\Omega_{out,v}, \Omega_{in,u}) = \mathbf{a}(\Omega_{out,v}) \odot \mathbf{a}(\Omega_{in,u}), \quad \text{for } u, v = 1, \ldots N, \tag{6}$$

which means the equivalent steering vector or channel response from the transmitter at $\Omega_{in,u}$ to the receiver at $\Omega_{out,v}$. Therefore, equation (5) can be represented in an equivalent way as

$$\hat{y}_{r,i} = \mathbf{w}^H \mathbf{A}_{C,i}\mathbf{s} + n_i, \quad i = 1, 2, \ldots, N. \tag{7}$$

$\hat{y}_{r,i}$ is the phased signal received by i-th receiver Rx_i, $\mathbf{w}$ is a column vector with its elements being the main diagonal elements of $\mathbf{W}$. It is worth mentioning that $\mathbf{w}$ is the *single* weight vector employed on the surface to achieve *all* transceiver pairs' desired signal response and mutual interference suppression simultaneously. n_i is the noise at Rx_i, and $\mathbf{A}_{C,i}$ is the combined steering matrix for i-th receiver which can be expressed as

$$\mathbf{A}_{C,i} = [\mathbf{a}_C(\Omega_{out,i}, \Omega_{in,1}), \ldots, \mathbf{a}_C(\Omega_{out,i}, \Omega_{in,N})] \in \mathbb{C}^{M\times N}. \tag{8}$$

With respect to the i-th receiver, according to equations (7) and (8), the received signal is a mixture of signals from all directions including both the desired signal and interference, where only $\mathbf{a}_C(\Omega_{out,i}, \Omega_{in,i})$ corresponds to desired signal direction and other terms in $\mathbf{A}_{C,i}$ correspond to interference for Rx_i. Base on equation (7), the SINR for the receiver of i-th pair can be represented as

$$SINR_i = \frac{|\mathbf{w}^H \mathbf{a}_C(\Omega_{out,i}, \Omega_{in,i})|^2}{\sigma^2 + \sum_{j=1, j\neq i}^{N} |\mathbf{w}^H \mathbf{a}_C(\Omega_{out,i}, \Omega_{in,j})|^2}, \quad i = 1, 2, \ldots, N, \tag{9}$$

where σ^2 is the power of noise.

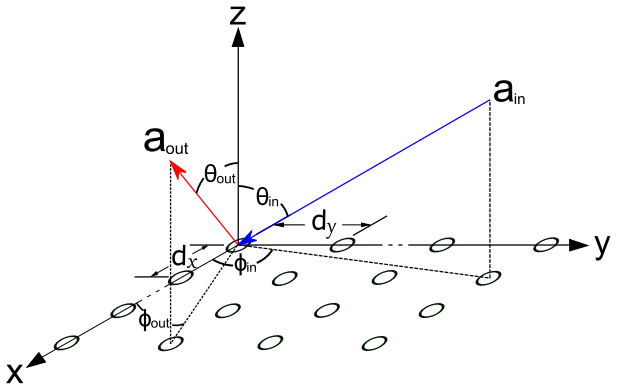

Fig. 2. 2D IRS under URA deployment in 3D geometry axis.

B. Steering Vector of ULA

Though the shape of surface and the arrangement of the elements on the surface can be arbitrary, however, we need to consider some regular IRSs in practical deployment and production. In the next sub-section, we will consider two of the most commonly used structures, i.e., ULA and URA, for analysis in Section IV. Again, it is mentioning that our model in this section and optimization in Section III are not limited by these specific structures.

For ULA, both $\Omega_{in,u}$ and $\Omega_{out,v}$ contain only azimuth angle that $\Omega_{in,u} = \phi_{in,u}$, $\Omega_{out,v} = \phi_{out,v}$ and $\phi_{in,u}, \phi_{out,v} \in [0, \pi]$, thus we can rewrite (2) as

$$\mathbf{A}_{\mathbf{in}} = \begin{bmatrix} 1 & \cdots & 1 \\ e^{-jkd\cos\phi_{in,1}} & \cdots & e^{-jkd\cos\phi_{in,N}} \\ \vdots & \ddots & \vdots \\ e^{-jkd\cos\phi_{in,1}(M-1)} & \cdots & e^{-jkd\cos\phi_{in,N}(M-1)} \end{bmatrix}. \tag{10}$$

Equation (6) can be rewritten as

$$\mathbf{a}_C(\phi_{out,v}, \phi_{in,u}) = [1, e^{-jkd(\cos\phi_{in,u} + \cos\phi_{out,v})}, \ldots, e^{-jkd(\cos\phi_{in,u} + \cos\phi_{out,v})(M-1)}]^T, \tag{11}$$

where $k = 2\pi/\lambda$ is the angular wavenumber, with λ being the wavelength of the signal. And d is the distance between the center of the adjacent electronic elements on the surface.

C. Steering Vector of URA

Consider the elements deployment on IRS as shown in Fig 2. There are M elements in total. M_x is the number of

elements along the X-axis and M_y is that of along the Y-axis, i.e., $M = M_x \cdot M_y$. d_x and d_y are elements distance along X-axis and Y-axis respectively. In this case, both $\Omega_{in,u}$ and $\Omega_{out,v}$ contain azimuth angle and elevation angle that $\Omega_{in,u} = (\phi_{in,u}, \theta_{in,u})$, $\Omega_{out,v} = (\phi_{out,v}, \theta_{out,v})$, $\phi_{in,u}, \phi_{out,v} \in [0, 2\pi]$ and $\theta_{in,u}, \theta_{out,v} \in [0, \pi/2]$. As the mutual coupling effect could be apparent when the element distance is less than half wavelength, one intuitive way to combine coupling effect is leveraging the statistical model. E.g, consider $\mathbf{w}$ as a vector of true value after coupling effect and it can be written as $\mathbf{w} = \mathbf{M}\mathbf{w}_{\text{theo}}$, where $\mathbf{w} = [w_1^*, \ldots, w_M^*]^H$, $\mathbf{w}_{\text{theo}}$ is the theoretical weights before mutual coupling and the mutual coupling matrix $\mathbf{M}$ can be considered as [43]

$$\mathbf{M}_{ij} = \frac{100^{-d_{i,j}/\lambda}}{\sum_{l=1}^{M} 100^{-d_{i,l}/\lambda}}. \tag{12}$$

where $d_{i,j}$ is the distance between i-th element and j-th element of the IRS. The corresponding form of compound steering vector for URA can be written as (13), shown at the bottom of the page, where $m_x \in (0, M_x - 1), m_y \in (0, M_y - 1)$. In addition

$$\begin{aligned} &f_{cs}(\Omega_{out,v}, \Omega_{in,u}) \\ &\quad = f_{cs}(\phi_{out,v}, \theta_{out,v}, \phi_{in,u}, \theta_{in,u}) \\ &\quad = \cos\phi_{out,v} \sin\theta_{out,v} + \cos\phi_{in,u} \sin\theta_{in,u}, \end{aligned} \tag{14}$$

$$\begin{aligned} &f_{ss}(\Omega_{out,v}, \Omega_{in,u}) \\ &\quad = f_{ss}(\phi_{out,v}, \theta_{out,v}, \phi_{in,u}, \theta_{in,u}) \\ &\quad = \sin\phi_{out,v} \sin\theta_{out,v} + \sin\phi_{in,u} \sin\theta_{in,u}. \end{aligned} \tag{15}$$

Compared with the form of ULA, it contains one more dimension of information of space, which is the elevation angle θ.

III. Proposed IRS Beamforming Weights

A. Optimal Weights of IRS for Multi-User

As managing the interference is critical for MU transmission, we propose to obtain the optimal solution to minimize the interference for IRS multi-user system through the multi-user linearly constrained minimum variance (MU-LCMV) beamformer. As a result, not only the known interference is nullified but that of from unknown directions is also minimized. In addition, LCMV is used since it is a class of common beamformer which can obtain the optimal result as a benchmark [44].

In particular, the optimization problem of minimizing interference can be formulated as

$$(\text{P1}): \quad \min J(\mathbf{w}) = E\{\Sigma_{i=1}^{N} |\hat{y}_{r,i}|^2\} \triangleq \mathbf{w}^H \mathbf{R} \mathbf{w} + \mathbf{I} N \sigma_n^2 \tag{16}$$

$$s.t.\ \mathbf{C^H w} = \mathbf{f}. \tag{17}$$

Equation (16) means to minimize overall power at all receivers and (17) refers to the constraint equations for all transceiver pairs. σ_n^2 is the power of noise and we assume it is the same at all receivers. The $\mathbf{R}$ in (16) is the covariance matrix and can be written as

$$\mathbf{R} = \mathbf{A}_C \mathbf{A}_C^H, \tag{18}$$

where $\mathbf{A}_C$ that containing all critical steering vectors is written, via concatenation of each steering matrix in equation (8) for N receivers, as

$$\begin{aligned} \mathbf{A}_C = \Bigg[&\underbrace{\mathbf{a}_C(\Omega_{out,1}, \Omega_{in,1}), \ldots \mathbf{a}_C(\Omega_{out,1}, \Omega_{in,N})}_{\text{N}}, \\ &\underbrace{\ldots}_{\text{N(N-2)}} \underbrace{\mathbf{a}_C(\Omega_{out,N}, \Omega_{in,1}), \ldots, \mathbf{a}_C(\Omega_{out,N}, \Omega_{in,N})}_{\text{N}} \Bigg] \\ &\in \mathbb{C}^{M \times N^2}, \end{aligned} \tag{19}$$

The $\mathbf{C}$ in (17) is the constraint matrix and can be expressed as

$$\mathbf{C} = [\mathbf{C}_1, \mathbf{C}_2], \tag{20}$$

$$\mathbf{C}_1 = [\mathbf{a}_C(\Omega_{out,1}, \Omega_{in,1}), \ldots, \mathbf{a}_C(\Omega_{out,N}, \Omega_{in,N})], \tag{21}$$

$$\begin{aligned} \mathbf{C}_2 = [\ldots, \mathbf{a}_C(\Omega_{out,q}, \Omega_{in,p}), \ldots], \\ p \neq q, \quad p = 1, \ldots, N, \ q = 1, \ldots, N, \end{aligned} \tag{22}$$

where $\mathbf{C}_1$ means the channel matrix which contains the steering vectors of desired signals to be remained, and $\mathbf{C}_2$ is the interference channel matrix composed of steering vectors of the unwanted directions where the signal will be suppressed. In addition, $\mathbf{f}$ is the beam pattern response constraint vector which contains two parts defined as

$$\mathbf{f} = [\mathbf{f}_1, \mathbf{f}_2]^T, \tag{23}$$

$$\mathbf{f}_1 = \left[\underbrace{\delta_{11}, \ldots, \delta_{NN}}_{N} \right]^T, \tag{24}$$

$$\mathbf{f}_2 = \left[\underbrace{\ldots, \delta_{pq}, \ldots}_{N(N-1)} \right]^T. \tag{25}$$

The $\mathbf{f}_1$ is corresponding the response values for desired signals, while $\mathbf{f}_2$ contains the maximum tolerant response value for interference. For simplicity but without loss of generality, the value can be set to unit power response, i.e., $\delta_{ii} = \delta_{lower} = 1$, for all desired signal (i.e., the minimum achieved power response at the desired directions) as a lower bound. To suppress the interference, we can set $\delta_{pq} = \delta_{upper} \ll \delta_{lower}$, which means δ_{upper} is an upper bound of the interference response.

The optimal solution of (P1) can be derived base on the mindset of the well-known LCMV beamformer with the Lagrange method [45].

$$\mathbf{w}_{opt} = \mathbf{R^{-1}C}(\mathbf{C}^H \mathbf{R}^{-1} \mathbf{C})^{-1} \mathbf{f}. \tag{26}$$

$$\begin{aligned} \mathbf{a}_C(\Omega_{out,v}, \Omega_{in,u}) = [1, e^{-jk(f_{cs}(\Omega_{out,v}, \Omega_{in,u}) d_x(0) + f_{ss}(\Omega_{out,v}, \Omega_{in,u}) d_y(1))} \ldots, e^{-jk(f_{cs}(\Omega_{out,v}, \Omega_{in,u}) d_x m_x + f_{ss}(\Omega_{out,v}, \Omega_{in,u}) d_y m_y)}, \\ \ldots, e^{-jk(f_{cs}(\Omega_{out,v}, \Omega_{in,u}) d_x(M_x - 1) + f_{ss}(\Omega_{out,v}, \Omega_{in,u}) d_y(M_y - 1))}]^T \end{aligned} \tag{13}$$

To be noted that the optimization problem (P1) minimizes the sum power of interference at all receivers. Specifically, (P1) is to minimize the sum power of signals received by all receivers. However, the desired signal power component is kept constant through the constraint equation (17). Thus, it is equivalently that the interference are nullified by IRS. Although the weight is in the form of a single vector, the IRS can support multi-stream transmission since it is fundamentally different from the traditional MIMO system. We can prove mathematically that the IRS model with a single weight vector can be transferred to an equivalent traditional MIMO model with multiple weight vectors, subject to two conditions as follows. Firstly, the sufficient number of elements on the IRS should be equal or greater than the number of pairs, i.e., $M \geq N$. This condition guarantees there is a sufficient degree of freedom for achieving zero-forcing at the interference locations. It is worth noting that to make the system better performed, we typically require $M \geq N^2$. While this requirement can be easily achieved in practical deployment since each IRS can be with hundreds or thousands of elements. Secondly, the directions of receivers and transmitters should be different to each other, i.e., $\mathbf{A}_{C,i} \neq \mathbf{A}_{C,j}$, for $i \neq j$, and $i, j \in [1, N]$. This condition can assure the coefficient matrix of weights vector for zero-forcing is full rank. Under these two conditions, the manipulation by the common weight to different steering matrices would produce equivalent effects that different weight vectors manipulate the same steering matrix. Thus, multi-stream data transmission can be supported by a single IRS. The closed-form optimal solution in equation (26) achieves the required responses at the desired signal and interference directions. This AUPC solution provides an analytical upper bounds of performance and can guide the real system design. However, such a solution is ideal and impractical for IRS since the calculated weights in $\mathbf{w}$ can have arbitrary large (or small) amplitude, which is impossible for a passive IRS where the amplitude is normally pre-designed and non-tunable. For this practical concern, we add the constant modulus constraint in the following problem. Though amplitude variation is an issue of designing the weights, relative methods can be applied to equalize the variation which will be studied in the future work.

B. Suboptimal Weights With Constraints

As it is a passive reflector, the amplitude of each element typically equals to or less than 1, depends on the design materials and circuits. Besides, in a practical IRS, all elements are periodically deployed on the surface with the same reflecting coefficients (i.e., they have the same amplitude). For simplicity and without losing the generality, the amplitude of weights is fixed to 1 in this paper.

To solve the problem with the new constraint, let $\mathbf{w} = [w_1, \ldots, w_M]^H$ where $w_m = e^{j\theta_m}, \theta_m \in (0, 2\pi], \forall m = 1, \ldots, M$. We propose using sequential quadratic programming (SQP) [46] to get ACPC solution by solving following problem

$$(\text{P2}): \min_{\mathbf{w}} J(\mathbf{w}) = E\{\Sigma_{i=1}^{N} |\hat{y}_{r,i}|^2\} \triangleq \mathbf{w}^H \mathbf{R} \mathbf{w} \tag{27}$$

$$s.t.\ \mathbf{C}_1^H \mathbf{w} \geq \mathbf{f}_1, \tag{28}$$

$$\mathbf{C}_2^H \mathbf{w} \leq \mathbf{f}_2, \tag{29}$$

$$w_m = e^{j\theta_m}, \quad \theta_m \in (0, 2\pi],\ m = 1, \ldots, M. \tag{30}$$

To be noted, (P2) with nonlinear constraints is not convex due to the constraint of constant modulus is introduced, therefore, (P2) is NP-hard. We propose to use the SQP method, which is a class of popular method for solving nonlinear and nonconvex optimization, to provide a locally optimal result for our work. The biggest advantage is that it can search the infeasible points, which can be useful when constraints become strict such that other algorithms cannot obtain a solution normally. As equation (30) should be satisfied to avoid the unbounded minimization of original problem via SQP, we substitute $\mathbf{w}$ with $\boldsymbol{\theta}$, where $\boldsymbol{\theta} = [\theta_1, \ldots, \theta_M]^T$, in (P2) to optimize the the phase directly using the mapping relationship of equation (30). Then, SQP solves (P2) by solving a quadratic programming subproblem first in each iteration to compute a search direction for (P2). Each subproblem is obtained by linearising the constraints and approximating the Lagrangian function as

$$L(\boldsymbol{\theta}, \boldsymbol{\lambda}) = J(\boldsymbol{\theta}) - \sum_{i=1}^{N^2} \lambda_i G_i(\boldsymbol{\theta}), \tag{31}$$

where $\boldsymbol{\lambda} = [\lambda_1, \ldots, \lambda_l]^T \in \mathbb{R}^{N^2}$ is the vector of the Lagrange multiplier. G_i represent i-th constraint in (28) and (29). And the subproblem to be solved to find a search direction for original problem (P2) can be expressed as

$$(\text{P3}): \min \frac{1}{2} \mathbf{d}(k)^T \mathbf{B}(k) \mathbf{d}(k) + \mathbf{g}^T \mathbf{d}(k) \tag{32}$$

$$s.t.\ G_i + \nabla G_i^T \mathbf{d}(k) \geq 0 \quad i = 1, 2, \cdots N^2, \tag{33}$$

where $\mathbf{g} = \nabla J(\boldsymbol{\theta}), G_i = G_i(\boldsymbol{\theta})$ and $\mathbf{B}(k)$ is usually a positive definite approximation to the Hessian matrix of the Lagrangian function with respect to $\boldsymbol{\theta}$. $\mathbf{d}(k)$ is the solution to search a $(k+1)$-th iterated solution of (P2) at k-th iteration, which can be used as

$$\boldsymbol{\theta}(k+1) = \boldsymbol{\theta}(k) + a_k \mathbf{d}(k), \tag{34}$$

where $a_k \in (0, 1]$ is the step length parameter. Next, to guarantee the global convergence of (P2), a merit function is constructed as

$$\eta(\theta) = J(\boldsymbol{\theta}) + p||\mathbf{G}^+(\boldsymbol{\theta})||_1, \quad p > 0 \tag{35}$$

where $J(\boldsymbol{\theta})$ is the objective function of (P2) after substitution of $\mathbf{w}$ with $\boldsymbol{\theta}$. The i-the term of $\mathbf{G}^+(\boldsymbol{\theta})$ is

$$G_i^+(\boldsymbol{\theta}) = \begin{cases} 0 & \text{if} \quad G_i(\boldsymbol{\theta}) \leq 0 \\ G_i(\boldsymbol{\theta}) & \text{if} \quad G_i(\boldsymbol{\theta}) > 0, \end{cases} \quad i = 1, 2, \ldots, N^2. \tag{36}$$

Thus, a_k can be computed by using the line search method in the direction provided by the solution of (P3) to minimize the value of merit function $\eta(\boldsymbol{\theta})$ at k-th iteration. Once the minimum of merit function is reached, we obtain $\boldsymbol{\theta}^*$ and $\mathbf{w}^*$ to (P2).

SQP algorithm is defined as: Step 1, initialize θ, and k. Step 2, solve the subproblem (P3) to determine $\mathbf{d}(k)$ and let $\boldsymbol{\lambda}_{k+1}$ be the vector of the Lagrange multiplier of the linear constraints obtained from the subproblem (P3). Step 3, compute the length a_k such that $\eta(\theta(k) + a_k \mathbf{d}(k)) < \eta(\theta(k))$

then update the solution by equation (34). Step 4, calculate $\mathbf{B}(k+1)$ from $\mathbf{B}(k)$ using a quasi-Newton formula. Step 5, stop until $||\eta(\theta(k+1)) - \eta(\theta(k))||_1 < \epsilon$ is achieved, where $\epsilon > 0$. Otherwise, go back to Step 2.

C. Limitation of Single IRS Assisted Communication System

Since the multi-user transmission is achieved by a single IRS, fundamental limits on the transceiver locations can be defined by the following corollary.

Corollary 1: Directions of different transmitters should not be the same, and so as to directions of receivers, which can be represented as

$$\Omega_{in,1} \neq \Omega_{in,2} \neq \cdots \neq \Omega_{in,N} \ and \\ \Omega_{out,1} \neq \Omega_{out,2} \neq \cdots \neq \Omega_{out,N}. \quad (37)$$

This condition can be verified easily through the constraints of the original optimization problem. Taking $N = 2$ as an example, `Tx1` sends signal to `Rx1` and `Tx2` sends signal to `Rx2`. According to the formulation (27), the solution should satisfy constraints (29) and (30) for specific responses and then we have relationships by rewritten the constraints as

$$\begin{cases} \mathbf{w}_{opt}^H \mathbf{a}_C(\Omega_{out,1}, \Omega_{in,1}) \geq \delta_{lower} \\ \mathbf{w}_{opt}^H \mathbf{a}_C(\Omega_{out,2}, \Omega_{in,1}) \leq \delta_{upper} \\ \mathbf{w}_{opt}^H \mathbf{a}_C(\Omega_{out,2}, \Omega_{in,2}) \geq \delta_{lower} \\ \mathbf{w}_{opt}^H \mathbf{a}_C(\Omega_{out,1}, \Omega_{in,2}) \leq \delta_{upper}, \end{cases} \quad (38)$$

where $\delta_{lower} \gg \delta_{upper}$. If $\Omega_{in,1} = \Omega_{in,2}$, by substituting $\Omega_{in,2}$ with $\Omega_{in,1}$, equation (38) becomes

$$\begin{cases} \mathbf{w}_{opt}^H \mathbf{a}_C(\Omega_{out,1}, \Omega_{in,1}) \geq \delta_{lower} \\ \mathbf{w}_{opt}^H \mathbf{a}_C(\Omega_{out,1}, \Omega_{in,1}) \leq \delta_{upper} \\ \mathbf{w}_{opt}^H \mathbf{a}_C(\Omega_{out,2}, \Omega_{in,1}) \leq \delta_{upper} \\ \mathbf{w}_{opt}^H \mathbf{a}_C(\Omega_{out,2}, \Omega_{in,1}) \geq \delta_{lower}. \end{cases} \quad (39)$$

Considering that the minimum response of desired signal δ_{lower} is normally much larger than the maximum response of interference δ_{upper}, i.e., $\delta_{lower} \gg \delta_{upper}$, the first and the second equations (also the third and fourth) of (39) are self contradicted. The condition of transmitters at the same direction makes original optimization problem unsolvable. The verification is the same if receivers are at the same direction.

According to **Corollary 1**, it is not difficult to conclude that if incident angles or exit angles are too close to each other, low channel signal-to-interference-plus-noise ratio (SINR) will be achieved. However, these limitations can be overcome by using more than one IRS to make transceiver pairs spatially distinguishable. In a nutshell, for a single meta-surface system to realize multi-user transmission, no overlapping in terms of both transmitters' and receivers' directions is compulsory.

IV. Redundant Beam

Based on the model given by Section II and the optimization problem formulation in Section III, it is not difficult to imagine IRS works as a special "mirror" in which each `Tx` can "see" its targeted `Rx` through such a mirror. In addition, since there is only one set of weights for all transceivers, each transmitter will be able to "see" another $N-1$ redundant beams. Given the fixed weights, moving the observation location from one transmitter to another (e.g., the 2nd transmitter) will "see" its beam but not new generated beam (and we cannot since only has one set of weights). Equivalently, it shifts the 1st pair's one of the redundant beams as its main beam for another receiver. In other words, the beam pattern of each pair should have in total N peaks with one main beam at the desired direction and another $N-1$ redundant beams in other directions if redundant beams are judged to be exist. In addition, each direction of redundant beams is only determined by the direction of such a pair and another pair (i.e., one of redundant beams for q-th `Tx` and `Rx` is determined by the directions of p-th `Tx` and `Rx`). The redundant beam can be determined by extending the Bragg condition with one more incident/exit angular parameter due to the reflection of EM wave is considered, instead of just one way beam transmitting/receiving [47]. Next, we mathematically derive the directions of redundant beams under different element distances. It is worth mentioning that the derivations in Section II and III apply to any arbitrary geometrical shape of IRS. However, to make the discussion simple and easy to follow, we specify our discussion with a ULA IRS and then extend it to URA IRS.

To investigate the relationship between the direction of the redundant beam and direction of transceiver pairs, we divide our discussion into three cases according to the range of element distance. It should be mentioned that in this paper, we discuss the cases that $d \in (0, \lambda/2]$. The scenario of $d \in (\lambda/2, \infty)$ is not considered here for both ULA and URA, since it may cause signal spatial aliasing. We denote the direction of a specific redundant beam as $\Omega_{RB,pq}$ which means that the q-th receiver can receive a signal from q-th transmitter at $\Omega_{RB,pq}$, and such a direction is essentially caused by the p-th pair's constraint. Appendix A list the proofs of following corollaries for both ULA and URA.

A. Beam Pattern of IRS for Multi-User

Beam pattern is an ideal metric to measure the performance of the interference cancellation and observe redundant beams. Based on the combined steering vector of $\Omega_{in,u}$ and $\Omega_{out,v}$, the beam pattern of the IRS based beamformer can be obtained and written as

$$B(\Omega_{out,v}, \Omega_{in,u}) = |\mathbf{w}^H \mathbf{a}_C(\Omega_{out,v}, \Omega_{in,u})|. \quad (40)$$

Note that the weight vector $\mathbf{w}$ can be either ideal or practical weights calculated from different optimizations formulated in Section III. The beam pattern $B(\Omega_{out,v}, \Omega_{in,u})$ can be regarded as the performance metric to describe the sensitivity of meta-surface with respect to the signal transmitted and received from different angles of arrival (AOA).

B. Redundant Beam of ULA

We define $\gamma_{pq} = \cos\phi_{in,p} + \cos\phi_{out,p} - \cos\phi_{in,q}$. Given $\phi_{in}, \phi_{out} \in [0, \pi]$, we have $\gamma_{pq} \in [-3, 3]$. It is an intermediate variable directly relate to $\Omega_{RB,pq}$ and the derivation can refer to Appendix A.

TABLE I
$\Omega_{RB,pq}$ OF URA WITH $d = \lambda/2$, COROLLARY 5

$\phi_{pq} \in [0, 2\pi]$ \ β_{pq} / α_{pq}	[-3,-1]	(-1,1)	[1,3]
[-3,-1]	$\arctan(\frac{\beta_{pq}+2}{\alpha_{pq}+2}) + n_3\pi$	$\arctan(\frac{\beta_{pq}}{\alpha_{pq}+2}) + n_3\pi$	$\arctan(\frac{\beta_{pq}-2}{\alpha_{pq}+2}) + n_3\pi$
(-1,1)	$\arctan(\frac{\beta_{pq}+2}{\alpha_{pq}}) + n_3\pi$	$\arctan(\frac{\beta_{pq}}{\alpha_{pq}}) + n_3\pi$	$\arctan(\frac{\beta_{pq}-2}{\alpha_{pq}}) + n_3\pi$
[1,3]	$\arctan(\frac{\beta_{pq}+2}{\alpha_{pq}-2}) + n_3\pi$	$\arctan(\frac{\beta_{pq}}{\alpha_{pq}-2}) + n_3\pi$	$\arctan(\frac{\beta_{pq}-2}{\alpha_{pq}-2}) + n_3\pi$

β_{pq}	[-3,-1]	(-1,1)	[1,3]
$\theta_{pq} \in [0, \frac{\pi}{2}]$	$\arcsin(\frac{\beta_{pq}+2}{\sin\phi_{pq}})$	$\arcsin(\frac{\beta_{pq}}{\sin\phi_{pq}})$	$\arcsin(\frac{\beta_{pq}-2}{\sin\phi_{pq}})$

Corollary 2: Consider a ULA IRS with $d = \lambda/2$ for N pairs' transceivers. The redundant beam direction $\Omega_{RB,pq} = (\phi_{pq})$ can be calculated as follows

$$\phi_{pq} = \begin{cases} \arccos(\gamma_{pq}+2), & \gamma_{pq} \in [-3,-1] \\ \arccos(\gamma_{pq}-2), & \gamma_{pq} \in [1,3] \\ \arccos(\gamma_{pq}), & \gamma_{pq} \in (-1,1) \\ 0 \ and \ \pi, & \gamma_{pq} = -1 \ or \ 1. \end{cases} \tag{41}$$

Equation (41) shows that $\Omega_{RB,pq}$ is decided by value of γ_{pq} which is determined by specific directions of considered transceiver pairs. Since redundant beams are caused by inter-pairs' directions relationship, the redundant beams for other pairs can also be calculated using those pairs' directions. Next, let us consider elements distance $d \in (0, \lambda/4)$ and $d \in [\lambda/4, \lambda/2)$, respectively.

Corollary 3: Consider a ULA IRS with $d \in (0, \lambda/4)$ for N pairs' transceivers,

$$\phi_{pq} = \begin{cases} \arccos(\gamma_{pq}), & \gamma_{pq} \in [-1,1] \\ \emptyset, & else \end{cases} \tag{42}$$

Note that when γ_{pq} is not in the range of $[-1,1]$, there is no redundant beam. The rationale behind is that with sufficiently large compound channel differences of two pairs, the manipulative effect from weights is sufficiently different, and so as to power allocation result from IRS. If pairs are close to each other, high channel correlation causes similar beamforming results by weights. Since pairs still have to keep desired responses, then weights have to balance such constraint, so power is scattered, and as a result, redundant beams are produced.

Corollary 4: Consider a ULA IRS with $d \in [\lambda/4, \lambda/2)$ for N pairs' transceivers, ϕ_{pq} can be expressed as

$$\phi_{pq} = \begin{cases} \arccos(\gamma_{pq}), & \gamma_{pq} \in [-1,1] \\ \arccos(\gamma_{pq}+\lambda/d), & \gamma_{pq} \in [-3,-1], \ \lambda/d \le 1-\gamma_{pq} \\ \emptyset, & \gamma_{pq} \in [-3,-1], \ \lambda/d > 1-\gamma_{pq} \\ \arccos(\gamma_{pq}-\lambda/d), & \gamma_{pq} \in [1,3], \ \lambda/d \le 1+\gamma_{pq} \\ \emptyset, & \gamma_{pq} \in [1,3], \ \lambda/d > 1+\gamma_{pq} \end{cases} \tag{43}$$

Note that when γ_{pq} is not in the range of $[-1,1]$, the existence of redundant beam depends on the relationship between the specific value of γ_{pq} and ratio of wavelength and element distance.

C. Redundant Beam of URA

Consider a URA IRS with $d = \lambda/2$ and we define other two intermediate variables as

$$\begin{aligned} \alpha_{pq} &= \cos\phi_{in,p}\sin\theta_{in,p} + \cos\phi_{out,p}\sin\theta_{out,p} \\ &\quad - \cos\phi_{in,q}\sin\theta_{in,q}, \end{aligned} \tag{44}$$

$$\begin{aligned} \beta_{pq} &= \sin\phi_{in,p}\sin\theta_{in,p} + \sin\phi_{out,p}\sin\theta_{out,p} \\ &\quad - \sin\phi_{in,q}\sin\theta_{in,q}. \end{aligned} \tag{45}$$

Similar to ULA case, it is easy to find that both α_{pq} and $\beta_{pq} \in [-3,3]$. Then, we can have following corollaries.

Corollary 5: Consider a URA IRS with $d = \lambda/2$ for N pairs' transceivers. The redundant beam direction $\Omega_{RB,pq} = (\phi_{pq}, \theta_{pq})$ in this case, and it can be calculated from TABLE I. Here, $n_3 \in Z$.

For $d \in (0, \lambda/4)$ and $d \in [\lambda/4, \lambda/2)$, we have the following corollaries respectively.

Corollary 6: For URA IRS with $d \in (0, \lambda/4)$, the reflection angle of the redundant beam ϕ_{pq} and θ_{pq} can be expressed as

$$\phi_{pq} = \begin{cases} \arctan(\frac{\beta_{pq}}{\alpha_{pq}}), & \alpha_{pq}, \ \beta_{pq} \in [-1,1] \\ \emptyset, & else, \end{cases} \tag{46}$$

$$\theta_{pq} = \begin{cases} \arcsin(\frac{\beta_{pq}}{\sin\phi_{pq}}), & \alpha_{pq}, \ \beta_{pq} \in [-1,1] \\ \emptyset, & else. \end{cases} \tag{47}$$

Corollary 7: When $d \in [\lambda/4, \lambda/2)$, the reflect angle of the redundant beam ϕ_{pq} and θ_{pq} can be expressed in TABLE II.

Note that the redundant beam is a side effect of the IRS when multiple pairs of signals are reflected, and we have the following remarks.

Remark 1: With N pairs of transceivers, up to $N-1$ redundant beams can be generated by the optimal weights and thus may cause significant power loss. In worst-case scenarios, a multiplexing gain N can be achieved while the power efficiency will be $1/N$.

Remark 2: Under some specific transceivers' directions with relative small d, there is no redundant beams and thus the power of signal can be focused on the desired direction. However, with a small d, the beamforming resolution is not ideal as a large one.

V. SIMULATION RESULTS

In the simulations, we use an IRS composed of 16×16 elements with element distance of $d = \lambda/2$, unless otherwise

TABLE II

$\Omega_{RB,pq}$ OF URA WITH $d \in [\lambda/4, \lambda/2)$, COROLLARY 7

$\phi_{pq} \in [0, 2\pi]$ \ β_{pq} / α_{pq}	[-3,-1], $\beta_{pq} + \frac{2\pi}{kd} \leq 1$	(-1,1)	[1,3], $\beta_{pq} - \frac{2\pi}{kd} \geq -1$
[-3,-1], $\alpha_{pq} + \frac{2\pi}{kd} \leq 1$	$\arctan\left(\frac{\beta_{pq}+\frac{\lambda}{d}}{\alpha_{pq}+\frac{\lambda}{d}}\right) + n_3\pi$	$\arctan\left(\frac{\beta_{pq}}{\alpha_{pq}+\frac{\lambda}{d}}\right) + n_3\pi$	$\arctan\left(\frac{\beta_{pq}-\frac{\lambda}{d}}{\alpha_{pq}+\frac{\lambda}{d}}\right) + n_3\pi$
(-1,1)	$\arctan\left(\frac{\beta_{pq}+\frac{\lambda}{d}}{\alpha_{pq}}\right) + n_3\pi$	$\arctan\left(\frac{\beta_{pq}}{\alpha_{pq}}\right) + n_3\pi$	$\arctan\left(\frac{\beta_{pq}-\frac{\lambda}{d}}{\alpha_{pq}}\right) + n_3\pi$
[1,3], $\alpha_{pq} - \frac{2\pi}{kd} \geq -1$	$\arctan\left(\frac{\beta_{pq}+\frac{\lambda}{d}}{\alpha_{pq}-\frac{\lambda}{d}}\right) + n_3\pi$	$\arctan\left(\frac{\beta_{pq}}{\alpha_{pq}-\frac{\lambda}{d}}\right) + n_3\pi$	$\arctan\left(\frac{\beta_{pq}-\frac{\lambda}{d}}{\alpha_{pq}-\frac{\lambda}{d}}\right) + n_3\pi$

β_{pq}	[-3,-1], $\beta_{pq} + \frac{2\pi}{kd} \leq 1$	(-1,1)	[1,3], $\beta_{pq} - \frac{2\pi}{kd} \geq -1$
$\theta_{pq} \in [0, \frac{\pi}{2}]$	$\arcsin\left(\frac{\beta_{pq}+\frac{\lambda}{d}}{\sin\phi_{pq}}\right)$	$\arcsin\left(\frac{\beta_{pq}}{\sin\phi_{pq}}\right)$	$\arcsin\left(\frac{\beta_{pq}-\frac{\lambda}{d}}{\sin\phi_{pq}}\right)$

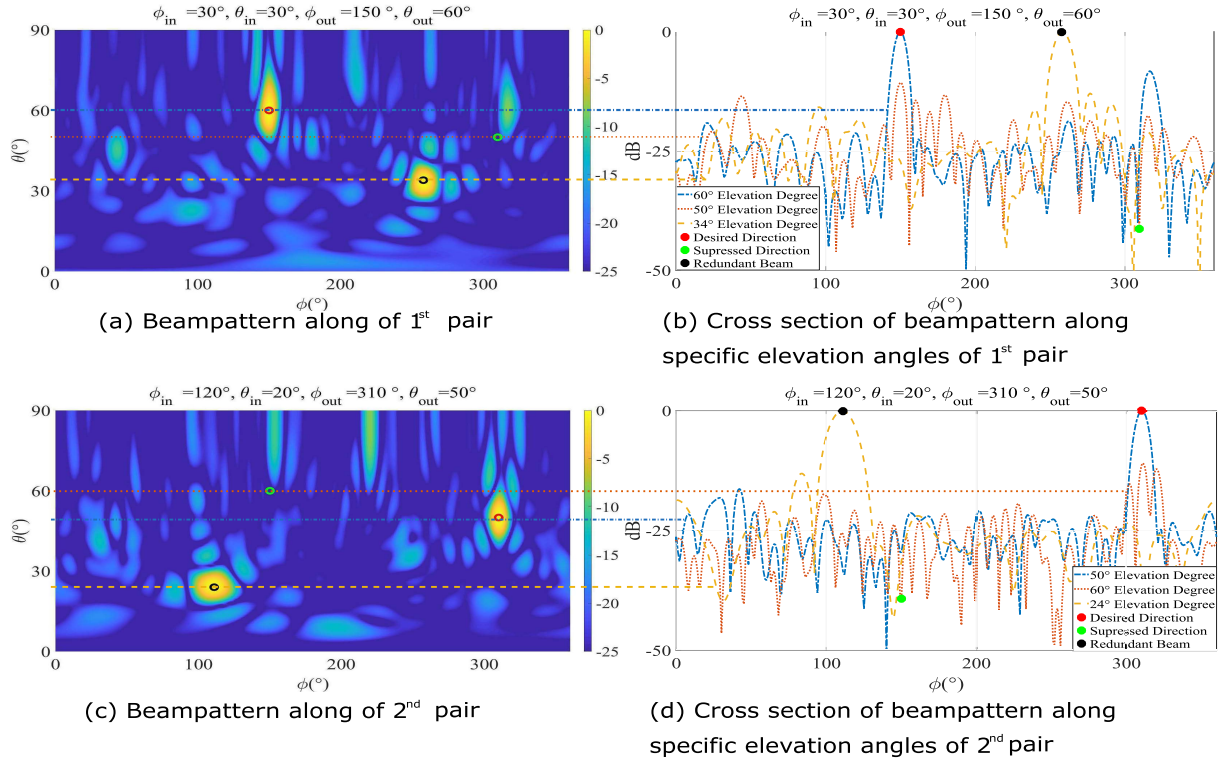

Fig. 3. Beampattern of ACPC solution. (a) Beampattern of 1st pair. (b) Cross section of 1st pair along elevation directions of signal of interest. (c) Beampattern of 2nd pair. (d) Cross section of 2nd pair along elevation directions of signal of interest. For the 1st pair, the three curves are about $\theta = 60°$, $50°$ and $34°$ respectively. For the 2nd pair, the three lines correspond to $\theta = 50°$, $60°$ and $24°$ respectively.

specified. All elements are isotropic and assumed to have the perfect reflective coefficient, i.e., $|w_m| = 1$. For all simulations, we assume that signal power is normalized and the additive noise at each receiver is set as -10 dB unless other specified. Two pairs of transceivers are considered in the simulations and their directions are $\Omega_{in,1} = (30°, 30°), \Omega_{out,1} = (150°, 60°), \Omega_{in,2} = (120°, 20°), \Omega_{out,2} = (310°, 50°)$ unless other specified.

A. Redundant Beams of URA Based on ACPC

Firstly, we consider the ACPC solution of the problem (27) calculated by the SQP algorithm. According to the corollaries proposed in this paper, we can analytically calculate that the redundant beam for 1st pair of the transceiver is at $\Omega_{RB,21} = (258.3°, 33.5°)$ and the redundant beam for 2nd pair is at $\Omega_{RB,12} = (110.6°, 24.4°)$. Fig. 3 shows simulation results. The main beam and redundant beam are presented in each sub-figure at left, respectively. As marked in the figure, each main beam is marked by a red circle, each redundant beam is marked by a black circle, and the interference position where needs to be suppressed to make interference-free is marked by a green circle. Through Fig. 3, more detailed for particular θ value can be observed from the beampattern. These figures are the cross-section along the elevation angle of the figures at the left-hand side, and the cut positions of interest have been marked by the dashed lines from the left figures, connected directly to the figures of the right-hand side. For figures at the right-hand side, the red dot marks the response at the desired direction, black dot marks the response

TABLE III
THE PERFORMANCE COMPARISON BETWEEN DIFFERENT ALGORITHMS

Noise power=10dB	Capacity (bps)		Signal Power(dB)		Interference(dB)	
Receiver	Rx1	Rx2	Rx1	Rx2	Rx1	Rx2
GA (ACPC)[48]	11.3	11.3	43.1	43.9	-12.3	-23.9
SQP (ACPC)	10.3	10.6	43.1	43.2	7.6	5.1
MU-LCMV-Phase (ACPC)	9.2	9.2	44.2	44.2	15.3	15.3
MU-LCMV-Amplitude (AXPC)	10.6	10.6	41.9	41.9	-246.3	-262.8

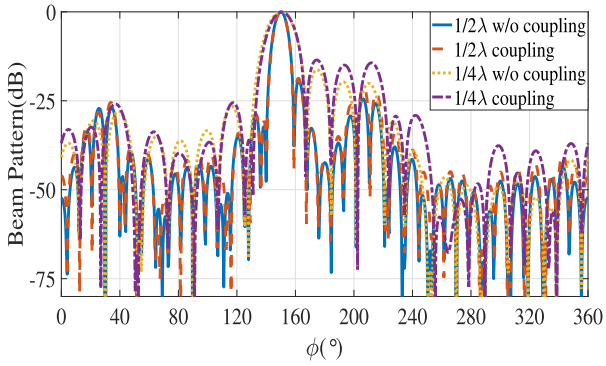

Fig. 4. Beam pattern with or without mutual coupling effect at $\theta = 60°$.

of redundant beam, and green dot marks the response at the suppressed direction. Therefore, it is not hard to find, through comparing the two figures at right-hand side, at where the main beam is generated in the direction where the 1st Rx is, the signal of 1st Tx received by the 2nd Rx is suppressed to around -41 dB, while at where that of main beam is generated for 2nd Rx, the signal from 2nd Tx received by 1st Rx is suppressed to about -39 dB, which is consistent to the desired characteristics of IRS system.

B. Mutual Coupling Effect on Sidelobes

To show the effect of mutual coupling on the side lobes of IRS system specifically, we leverage max ratio combining (MRC) algorithm [33] to obtain ACPC solution (by taking the phase of MRC directly) to maximize the SNR for only 1st pair user at $\Omega_{in,1} = (30°, 30°), \Omega_{out,1} = (150°, 60°)$. As shown in Fig. 4, the mutual coupling causes higher side lobes than that of without mutual coupling effect. With smaller element spacing, the higher side lobe can be observed on the beam pattern since sparsity in the mutual coupling matrix gets smaller when the element spacing gets smaller. Therefore, it is necessary to equalize the mutual coupling effect if the IRS leverage the small element spacing to reduce the power dispersion.

C. Multi-User Scenario of URA

In Fig. 5, we showcase the scenario of three pairs of transceivers. The new added 3rd pair transceiver is located at $\Omega_{in,3} = (190°, 50°)$ and $\Omega_{out,3} = (240°, 10°)$. For lowering side lobes on the beampattern, the optimal AUPC solution is implemented. We observe that by considering an extra 3rd pair transceiver, one more redundant beam is generated, and one more nullified direction is produced on the beampattern of $\mathtt{Tx}_1$ and $\mathtt{Tx}_2$ respectively. At the same time, the redundant beams caused by the constraints of the first two pairs remained at the same direction for $\mathtt{Tx}_1$ and $\mathtt{Tx}_2$. As for positions of redundant beams of 3rd pair transceiver, they can be calculated accurately using our corollary in Section IV.

D. The Performance Analysis of Proposed Algorithms

To analyze the performance of the proposed algorithms in Section III, the performances on the capacity, received power and interference are illustrated. In TABLE III, four algorithms are compared, and three algorithms are considered for solving the problem of ACPC for (P2). They are genetic algorithm (GA), SQP, and MU-LCMV-Phase which directly takes the phase of AUPC solution of (P1). MU-LCMV-Amplitude is shown for reference, which is obtained by normalizing the amplitude of the AUPC solution to provide the amplitude-relaxed phase-continuous solution (AXPC). Due to (P2) is NP-hard, the optimal solution is not available. Since GA is a class of exhaustive search method which can provide a nearly optimal solution where the local optima can be avoided by sufficient times of searching, we use GA as a near-global optimal benchmark. We can find the performance of capacity achieved by SQP is slightly lower than the benchmark GA, where the difference for capacity is less than 10% from the benchmark. However, GA's searching cost is much higher than other algorithms, which cannot be acceptable in real applications. To be noted, MU-LCMV-Phase and MU-LCMV-Amplitude achieve the highest received power and minimal interference power at receivers, respectively. Although MU-LCMV-Phase only achieves 80% percent capacity of GA, it is obtained analytically. MU-LCMV-Amplitude achieves interference-free transmission. It is worth mentioning that both MU-LCMV based solutions can be obtained with very low-complexity algorithms since they are based on the analytical solution.

Fig. 6(a) shows the error of redundant beam between the analytical calculation through **Corollary 5** and the simulation of AUPC and ACPC solutions. In this figure, lines drawn in the same color are under conditions of the same element distance of IRS but different solutions of the algorithm. As mentioned above, systems with small element distance have a worse resolution, so they are more likely to get a larger error on the direction of redundant beams. And the error reduces with the increase of elements, reaching a plateau at a range of large element number. In addition, AUPC outperforms ACPC on the accuracy performance.

E. SINR Performance

To show the robustness of the algorithm, this simulation evaluates the SINR performance versus the angles difference among the users. For simplicity, we use ULA IRS with 64 elements in this simulation. $\phi_{in,1} = 30°$ and $\phi_{out,1} = 100°$.

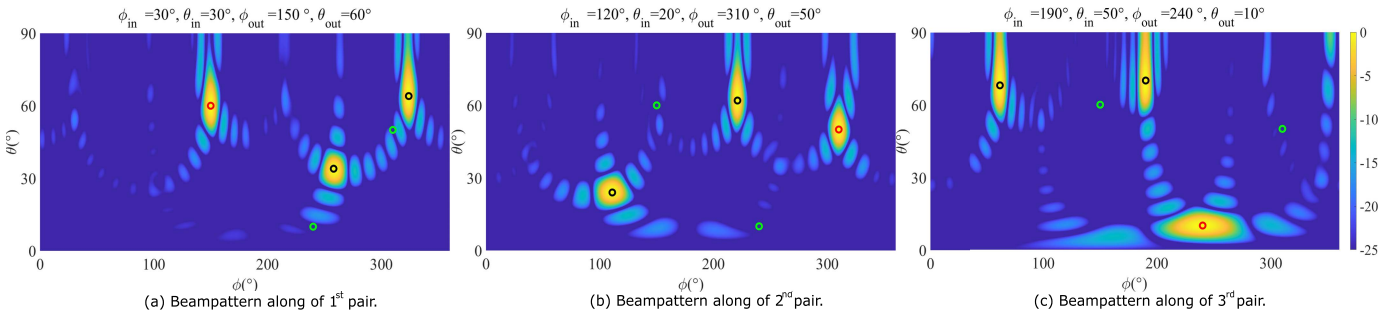

Fig. 5. Beampatterns of three pairs under AUPC solution. (a) Beampattern of 1st pair. (b) Beampattern of 2nd pair. (c) Beampattern of 3rd pair.

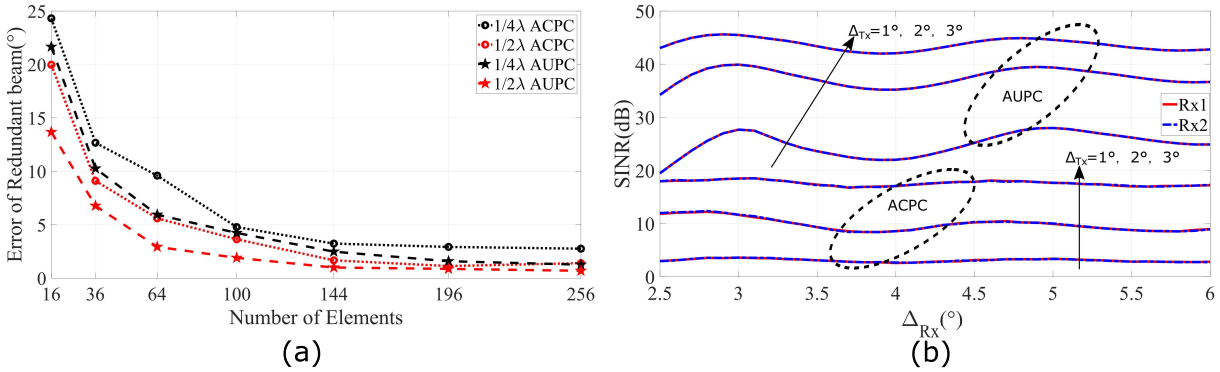

Fig. 6. (a) Redundant beam error between analytical calculation and simulation for different solutions. (b) SINR vs The angle difference of transmitters (and receivers).

The distance between each element is set to $\lambda/2$. We define $\Delta_{\text{Tx}} = \phi_{in,2} - \phi_{in,1}$ and $\Delta_{\text{Rx}} = \phi_{out,2} - \phi_{out,1}$ as the angle differences of transmitters and receivers respectively. As AUPC is unconstrained on amplitude, we define the norm of AUPC solution to be consistent with ACPC so they are on the same scale. As shown in the Fig. 6(b), with the angle difference of the transmitters Δ_{Tx} and receivers Δ_{Rx} increasing, the performance of SINR of both Rx1 and Rx2 are plotted. Their SINR improve and reach a peak value when angle difference is sufficiently large. The lines marked by same color are under same transceivers' position, and lines marked by same symbol are obtained by the same way of solution. Apparently, AUPC apparently outperforms ACPC on SINR. The fluctuation after the peak value is due to the spatial correlation between the merged steering vectors of the desired direction and interference direction varies. For results from AUPC weights, it realizes the optimal upper bound of SINR when the direction difference is large. While for ACPC, the upper bound is lower due to the amplitude of weights is constrained and thus beamforming angle resolution is limited. Therefore we can conclude that over close angles between each transmitter or receiver achieve low SINR. The error still exists as long as the number of elements is limited.

VI. Conclusion

Multi-user beamforming and transmission based on IRS is proposed in this paper. We model the channel and system for a single piece IRS. Optimization problems are formulated to obtain the optimal weight vector for different scenarios. A closed-form solution is first derived by using LCMV beamformer based on AUPC configuration. By constraining the amplitude and phase of the weight vector, ACPC solution is proposed for practical IRS implementation. A critical observation of the paper is that redundant beams exist in the system and brings significant power loss. We have mathematically analyzed the redundant beams under different IRS configurations to provide useful design guidance for analysis with more practical effect. Mutual coupling effect of IRS is also analyzed which indicate increasing on side lobes level with smaller element spacing. Results verified the finding and algorithms, and suggested to use a large angle difference between the transmitters (and receivers) for a good system performance.

Appendix A

Since **Corollary 2**, **Corollary 3**, and **Corollary 4** are based on ULA, due to the length limit of paper, we give the following proof of URA for its more general form.

A. Proof of Corollary 5

Consider $d = \lambda/2$ and URA IRS. Then equation (40) becomes:

$$\mathbf{B}(\Omega_{out,v}, \Omega_{in,u}) = \mathbf{B}(\phi_{out,v}, \theta_{out,v}, \phi_{in,u}, \theta_{in,u}), \tag{48}$$

$$\mathbf{B}(\Omega_{out,v}, \Omega_{in,u}) = \Big| \sum_{m_y=0}^{M_y-1} \sum_{m_x=0}^{M_x-1} w_{m_x m_y} \cdot e^{-jk(f_{cs}(\Omega_{out,v},\Omega_{in,u})d_x m_x + f_{ss}(\Omega_{out,v},\Omega_{in,u})d_y m_y)} \Big|. \tag{49}$$

For $N = 2$, from equation (28) and (29), the constraints can be expressed as follows

$$\begin{cases} \delta_{lower} \leq \mathbf{w}^T \mathbf{a}_C(\Omega_{out,1}, \Omega_{in,1}) \\ \quad = \mathbf{w}^T \mathbf{a}_C(\phi_{out,1}, \theta_{out,1}, \phi_{in,1}, \theta_{in,1}) \\ \delta_{lower} \leq \mathbf{w}^T \mathbf{a}_C(\Omega_{out,2}, \Omega_{in,2}) \\ \quad = \mathbf{w}^T \mathbf{a}_C(\phi_{out,2}, \theta_{out,2}, \phi_{in,2}, \theta_{in,2}) \\ \delta_{upper} \geq \mathbf{w}^T \mathbf{a}_C(\Omega_{out,2}, \Omega_{in,1}) \\ \quad = \mathbf{w}^T \mathbf{a}_C(\phi_{out,2}, \theta_{out,2}, \phi_{in,1}, \theta_{in,1}) \\ \delta_{upper} \geq \mathbf{w}^T \mathbf{a}_C(\Omega_{out,1}, \Omega_{in,2}) \\ \quad = \mathbf{w}^T \mathbf{a}_C(\phi_{out,1}, \theta_{out,1}, \phi_{in,2}, \theta_{in,2}) \end{cases} \tag{50}$$

Let

$$\begin{aligned} F_1(\Omega_{out,v}, \Omega_{in,u}) &= F_1(\phi_{out,v}, \theta_{out,v}, \phi_{in,u}, \theta_{in,u}) \\ &= e^{-j\pi f_{cs}(\phi_{out,v}, \theta_{out,v}, \phi_{in,u}, \theta_{in,u})}, \end{aligned} \tag{51}$$

$$\begin{aligned} F_2(\Omega_{out,v}, \Omega_{in,u}) &= F_2(\phi_{out,v}, \theta_{out,v}, \phi_{in,u}, \theta_{in,u}) \\ &= e^{-j\pi f_{ss}(\phi_{out,v}, \theta_{out,v}, \phi_{in,u}, \theta_{in,u})}. \end{aligned} \tag{52}$$

It is clear that the term $F_1(\Omega_{out,v}, \Omega_{in,u})$ and $F_2(\Omega_{out,v}, \Omega_{in,u})$ directly correlate to $\mathbf{a}_C(\Omega_{out,v}, \Omega_{in,u})$ from equation (13) since the multiplication of this two terms is the base of new merged steering vector. Thus, if the following relationship

$$F_1(\phi_{out,1}, \theta_{out,1}, \phi_{in,1}, \theta_{in,1}) = F_1(\phi_{12}, \theta_{12}, \phi_{in,2}, \theta_{in,2}) \tag{53}$$

and

$$F_2(\phi_{out,1}, \theta_{out,1}, \phi_{in,1}, \theta_{in,1}) = F_2(\phi_{12}, \theta_{12}, \phi_{in,2}, \theta_{in,2}) \tag{54}$$

hold, we have following equation

$$\mathbf{a}_C(\phi_{out,1}, \theta_{out,1}, \phi_{in,1}, \theta_{in,1}) = \mathbf{a}_C(\phi_{12}, \theta_{12}, \phi_{in,2}, \theta_{in,2}). \tag{55}$$

We can get

$$\delta_{lower} \leq \mathbf{w}^T \mathbf{a}_C(\phi_{12}, \theta_{12}, \phi_{in,2}, \theta_{in,2}), \tag{56}$$

which implies that the redundant beam of URA at ϕ_{12}, θ_{12}. And it is clear that if and only if equation (53) and (54) are both satisfied can both azimuth and elevation angle of redundant beam exist. It can be explained as the numerical equivalence of two merged steering vectors of the desired direction and the direction of redundant beam. As long as one constraint of steering vector is satisfied in one direction, this constraint would also affect another direction. In a general sense, any other steering vector which numerically equal to the constrained steering vectors of minimum secured power response would indicate redundant beams.

Next let's discuss the condition to make equation (53) and (54) hold respectively. To be noted that there is the periodicity of function F_1 and F_2 for its phasor form. If equation (53) and (54) hold, then it is necessary and sufficient that

$$\begin{aligned} &f_{cs}(\phi_{out,1}, \theta_{out,1}, \phi_{in,1}, \theta_{in,1}) + 2n_1 \\ &\qquad = f_{cs}(\phi_{12}, \theta_{12}, \phi_{in,2}, \theta_{in,2}), n_1 \in Z \end{aligned} \tag{57}$$

and

$$\begin{aligned} &f_{ss}(\phi_{out,1}, \theta_{out,1}, \phi_{in,1}, \theta_{in,1}) + 2n_2 \\ &\qquad = f_{ss}(\phi_{12}, \theta_{12}, \phi_{in,2}, \theta_{in,2}), n_2 \in Z \end{aligned} \tag{58}$$

hold respectively. Base on the definition of α_{12} and β_{12}, making equation (57) and (58) hold is equivalent to the following two equations

$$\alpha_{12} + 2n_1 = \cos\phi_{12} \sin\theta_{12}, n_1 \in Z, \tag{59}$$

$$\beta_{12} + 2n_2 = \sin\phi_{12} \sin\theta_{12}, n_2 \in Z, \tag{60}$$

have the correspondent solutions of ϕ_{12} and θ_{12}. Only under conditions of both left part of equation (59) and (60) have the value range of $[-1, 1]$ can they be solved out.

Specifically, when $\alpha_{12}, \beta_{12} \in [-3, -1]$, only if $n_1 = 1$, $n_2 = 1$, $-1 \leq \alpha_{12} + 2n_1 \leq 1$ and $-1 \leq \beta_{12} + 2n_2 \leq 1$ hold, $\phi_{12} = \arctan(\frac{\beta_{12}+2}{\alpha_{12}+2}) + n_3\pi, n_3 \in Z, \phi_{12} \in [0, 2\pi]$. Otherwise, ϕ_{12} does not exist. Then by further substituting ϕ_{12} into equation (60), $\theta_{12} = \arcsin(\frac{\beta_{12}+2}{\sin\phi_{12}}), \theta \in [0, \frac{\pi}{2}]$.

To be noted that there are usually two solutions of ϕ_{12} in this case. There might not be a correspondent solution of θ_{12} in which means the redundant beam does not exist. Likewise, the discussion on the condition of ϕ_{12} and θ_{12} can be concluded in TABLE I and TABLE II. Therefore, it can be summarized as **Corollary 5**.

From the results above, it provides the insight of of redundant beam. As we can find, the redundant beams are similar to the concept of grating lobes in the traditional antenna array theory. However, they are different and it might be tricky to distinguish those two concepts. I.e, the grating lobes are caused by large spacing between elements of antenna arrays such that the beamforming result can repeat in the angular domain of AOA/DOA more than once. For IRS, grating lobes are caused by large spacing between IRS element as well. However, due to IRS is equivalent to a cascading of antenna arrays, one more degree of freedom of AOA/DOA is introduced. E.g., for IRS in ULA, the "Bragg condition" can be written as

$$kd(\cos\theta_{out} + \cos\theta_{in}) = 2\pi n_0, \quad n_0 \in \mathbb{Z}, \tag{61}$$

where θ_{in} and θ_{out} are incident direction and exit direction respect to IRS for one pair transceiver. k and d are the wave number and spacing of elements respectively. The Bragg condition for traditional linear array is just

$$kd\cos\theta = 2\pi n_0, \quad n_0 \in \mathbb{Z}, \tag{62}$$

where θ can be transmit/receive direction of the ULA [47]. And it is not hard for us to find direction of transceivers and the element spacing jointly determining the existence of the "Bragg condition" for IRS in equation (61).

B. Proof of Corollary 6

Under condition of $d \in (0, \lambda/4)$, the equation (59) and (60) would be rewritten as

$$\alpha_{12} + \frac{2\pi n_1}{kd} = \cos\phi_{12} \sin\theta_{12}, \quad n_1 \in Z, \tag{63}$$

$$\beta_{12} + \frac{2\pi n_2}{kd} = \sin\phi_{12} \sin\theta_{12}, \quad n_2 \in Z, \tag{64}$$

which is the general form. The discussion on getting both ϕ_{12} and θ_{12} to make equation (63) and (64) hold is as follows.

When $\alpha_{12} \in [-1, 1]$ and $\beta_{12} \in [-1, 1]$. If $n_1 = 0$, $n_2 = 0$, $\phi_{12} = \arctan(\frac{\beta_{12}}{\alpha_{12}})$ and $\theta_{12} = \arcsin(\frac{\beta_{12}}{\sin\phi_{12}})$. If $n_1 \neq 0$ or

$n_2 \neq 0$, since $\alpha_{12} + \frac{2\pi n_1}{kd} \notin (-1, 1)$ or $\beta_{12} + \frac{2\pi n_2}{kd} \notin (-1, 1)$, both ϕ_{12} and θ_{12} would not exist.

Therefore, it can be summarized as **Corollary 6**.

C. Proof of Corollary 7

Consider URA IRS under condition of $d \in [\lambda/4, \lambda/2)$, the discussion of ϕ_{12} and θ_{12} base on value range of α_{12} and β_{12} to make equation (63) and (64) hold is as follows.

Case **1**, when $\alpha_{12} \in (-1, 1)$ and $\beta_{12} \in (-1, 1)$. If $n_1 = 0$, $n_2 = 0$, $\phi_{12} = \arctan(\frac{\beta_{12}}{\alpha_{12}})$ and $\theta_{12} = \arcsin(\frac{\beta_{12}}{\sin \phi_{12}})$. If $n_1 \neq 0$ or $n_2 \neq 0$, since $\alpha_{12} + \frac{2\pi n_1}{kd} \notin (-1, 1)$ or $\beta_{12} + \frac{2\pi n_2}{kd} \notin (-1, 1)$, both ϕ_{12} and θ_{12} would not exist.

Case **2**, when $\alpha_{12} \in [-3, -1]$ and $\beta_{12} \in [-3, -1]$. If $\alpha_{12} + \frac{2\pi}{kd} > 1$, $\alpha_{12} + \frac{2\pi n_1}{kd} > 1$ holds when $n_1 > 1$. And $\alpha_{12} + \frac{2\pi n}{kd} < -1$ holds when $n_1 < 1$. So when $\frac{\lambda}{d} > 1 - \alpha_{12}$, ϕ_{12} does not exist. And in another hand, when $\frac{\lambda}{d} > 1 - \beta_{12}$, θ_{12} does not exist as well.

Only if $\alpha_{12} + \frac{2\pi}{kd} \leq 1$ and $\beta_{12} + \frac{2\pi}{kd} \leq 1$, when $n_1 = 1$ and $n_2 = 1$, $\phi_{12} = \arctan(\frac{\beta_{12} + \frac{\lambda}{d}}{\alpha_{12} + \frac{\lambda}{d}}) + n_3\pi$ and $\theta_{12} = \arcsin(\frac{\beta_{12} + \frac{\lambda}{d}}{\sin \phi_{12}})$. Otherwise when $n_1 \neq 1$ or $n_2 \neq 1$, ϕ_{12} or θ_{12} do not exist since $\alpha_{12} + \frac{2\pi n_1}{kd} \notin (-1, 1)$ and $\beta_{12} + \frac{2\pi n_2}{kd} \notin (-1, 1)$.

Case **3**, when $\alpha_{12} \in [-3, -1]$ and $\beta_{12} \in (-1, 1)$. $\phi_{12} = \arctan(\frac{\beta_{12}}{\alpha_{12} + \frac{\lambda}{d}}) + n_3\pi$ and $\theta_{12} = \arcsin(\frac{\beta_{12}}{\sin \phi_{12}})$, under the condition that $\alpha_{12} + \frac{2\pi}{kd} \leq 1$.

Case **4**, when $\alpha_{12} \in [-3, -1]$ and $\beta_{12} \in [1, 3]$. $\phi_{12} = \arctan(\frac{\beta_{12} - \frac{\lambda}{d}}{\alpha_{12} + \frac{\lambda}{d}}) + n_3\pi$ and $\theta_{12} = \arcsin(\frac{\beta_{12} - \frac{\lambda}{d}}{\sin \phi_{12}})$, under the condition that $\alpha_{12} + \frac{2\pi}{kd} \leq 1$ and $\beta_{12} - \frac{2\pi}{kd} \geq -1$.

Case **5**, when $\alpha_{12} \in (-1, 1)$ and $\beta_{12} \in [-3, -1]$. $\phi_{12} = \arctan(\frac{\beta_{12} + \frac{\lambda}{d}}{\alpha_{12}}) + n_3\pi$ and $\theta_{12} = \arcsin(\frac{\beta_{12} + \frac{\lambda}{d}}{\sin \phi_{12}})$, under the condition that $\beta_{12} + \frac{2\pi}{kd} \leq 1$.

Case **6**, when $\alpha_{12} \in (-1, 1)$ and $\beta_{12} \in [1, 3]$. $\phi_{12} = \arctan(\frac{\beta_{12} - \frac{\lambda}{d}}{\alpha_{12}}) + n_3\pi$ and $\theta_{12} = \arcsin(\frac{\beta_{12} - \frac{\lambda}{d}}{\sin \phi_{12}})$, under the condition that $\beta_{12} - \frac{2\pi}{kd} \geq -1$.

Case **7**, when $\alpha_{12} \in [1, 3]$ and $\beta_{12} \in [-3, -1]$. $\phi_{12} = \arctan(\frac{\beta_{12} + \frac{\lambda}{d}}{\alpha_{12} - \frac{\lambda}{d}}) + n_3\pi$ and $\theta_{12} = \arcsin(\frac{\beta_{12} + \frac{\lambda}{d}}{\sin \phi_{12}})$, under the condition that $\alpha_{12} - \frac{2\pi}{kd} \geq -1$ and $\beta_{12} + \frac{2\pi}{kd} \leq 1$.

Case **8**, when $\alpha_{12} \in [1, 3]$ and $\beta_{12} \in (-1, 1)$. $\phi_{12} = \arctan(\frac{\beta_{12}}{\alpha_{12} - \frac{\lambda}{d}}) + n_3\pi$ and $\theta_{12} = \arcsin(\frac{\beta_{12}}{\sin \phi_{12}})$, under the condition that $\alpha_{12} - \frac{2\pi}{kd} \geq -1$.

Case **9**, when $\alpha_{12} \in [1, 3]$ and $\beta_{12} \in [1, 3]$. $\phi_{12} = \arctan(\frac{\beta_{12} - \frac{\lambda}{d}}{\alpha_{12} - \frac{\lambda}{d}}) + n_3\pi$ and $\theta_{12} = \arcsin(\frac{\beta_{12} - \frac{\lambda}{d}}{\sin \phi_{12}})$, under the condition that $\alpha_{12} - \frac{2\pi}{kd} \geq -1$ and $\beta_{12} - \frac{2\pi}{kd} \geq -1$. Therefore, it can be summarized as **Corollary 7**.

REFERENCES

[1] Y. Liu, L. Zhang, B. Yang, W. Guo, and M. A. Imran, "Programmable wireless channel for multi-user MIMO transmission using meta-surface," in *Proc. IEEE Global Commun. Conf. (GLOBECOM)*, Dec. 2019, pp. 1–6.

[2] T. S. Rappaport *et al.*, "Millimeter wave mobile communications for 5G cellular: It will work!" *IEEE Access*, vol. 1, pp. 335–349, 2013.

[3] L. Zhang, A. Ijaz, P. Xiao, M. M. Molu, and R. Tafazolli, "Filtered OFDM systems, algorithms, and performance analysis for 5G and beyond," *IEEE Trans. Commun.*, vol. 66, no. 3, pp. 1205–1218, Mar. 2018.

[4] J.-J. van de Beek, O. Edfors, M. Sandell, S. K. Wilson, and P. O. Borjesson, "On channel estimation in OFDM systems," in *Proc. IEEE 45th Veh. Technol. Conf.*, vol. 2, Jul. 1995, pp. 815–819.

[5] P. Schniter, "Low-complexity equalization of OFDM in doubly selective channels," *IEEE Trans. Signal Process.*, vol. 52, no. 4, pp. 1002–1011, Apr. 2004.

[6] Q. Liu, S. Zhou, and G. B. Giannakis, "Cross-layer combining of adaptive modulation and coding with truncated ARQ over wireless links," *IEEE Trans. Wireless Commun.*, vol. 3, no. 5, pp. 1746–1755, Sep. 2004.

[7] S. Catreux, V. Erceg, D. Gesbert, and R. W. Health, Jr., "Adaptive modulation and MIMO coding for broadband wireless data networks," *IEEE Commun. Mag.*, vol. 40, no. 6, pp. 108–115, Jun. 2002.

[8] A. Goldsmith, *Wireless Communications*. Cambridge, U.K.: Cambridge Univ. Press, 2005.

[9] H. Artes, D. Seethaler, and F. Hlawatsch, "Efficient detection algorithms for MIMO channels: A geometrical approach to approximate ML detection," *IEEE Trans. Signal Process.*, vol. 51, no. 11, pp. 2808–2820, Nov. 2003.

[10] T. L. Marzetta, "Massive MIMO: An introduction," *Bell Labs Tech. J.*, vol. 20, pp. 11–22, 2015.

[11] E. G. Larsson, O. Edfors, F. Tufvesson, and T. L. Marzetta, "Massive MIMO for next generation wireless systems," *IEEE Commun. Mag.*, vol. 52, no. 2, pp. 186–195, Feb. 2014.

[12] R. W. Heath, Jr., N. González-Prelcic, S. Rangan, W. Roh, and A. M. Sayeed, "An overview of signal processing techniques for millimeter wave MIMO systems," *IEEE J. Sel. Topics Signal Process.*, vol. 10, no. 3, pp. 436–453, Apr. 2017.

[13] F. Gao, B. Wang, C. Xing, J. An, and G. Y. Li, "Wideband beamforming for hybrid massive MIMO terahertz communications," *IEEE J. Sel. Areas Commun.*, vol. 39, no. 6, pp. 1725–1740, Jun. 2021.

[14] M. M. Molu, P. Xiao, M. Khalily, K. Cumanan, L. Zhang, and R. Tafazolli, "Low-complexity and robust hybrid beamforming design for multi-antenna communication systems," *IEEE Trans. Wireless Commun.*, vol. 17, no. 3, pp. 1445–1459, Mar. 2018.

[15] S. V. Hum and J. Perruisseau-Carrier, "Reconfigurable reflectarrays and array lenses for dynamic antenna beam control: A review," *IEEE Trans. Antennas Propag.*, vol. 62, no. 1, pp. 183–198, Jan. 2014.

[16] N. I. Zheludev and Y. S. Kivshar, "From metamaterials to metadevices," *Nature Mater.*, vol. 11, pp. 917–924, Nov. 2012.

[17] C. Huang, A. Zappone, G. C. Alexandropoulos, M. Debbah, and C. Yuen, "Reconfigurable intelligent surfaces for energy efficiency in wireless communication," *IEEE Trans. Wireless Commun.*, vol. 18, no. 8, pp. 4157–4170, Aug. 2019.

[18] Q. Wu and R. Zhang, "Intelligent reflecting surface enhanced wireless network via joint active and passive beamforming," *IEEE Trans. Wireless Commun.*, vol. 18, no. 11, pp. 5394–5409, Nov. 2019.

[19] M. Di Renzo *et al.*, "Smart radio environments empowered by reconfigurable AI meta-surfaces: An idea whose time has come," *EURASIP J. Wireless Commun. Netw.*, vol. 2019, no. 1, pp. 1–20, May 2019.

[20] H. Yang *et al.*, "A programmable metasurface with dynamic polarization, scattering and focusing control," *Sci. Rep.*, vol. 6, no. 1, Dec. 2016, Art. no. 35692.

[21] L. Zhang *et al.*, "Space-time-coding digital metasurfaces," *Nature Commun.*, vol. 9, no. 1, p. 4334, 2018.

[22] C. Liaskos, S. Nie, A. Tsioliaridou, A. Pitsillides, S. Ioannidis, and I. Akyildiz, "A new wireless communication paradigm through software-controlled metasurfaces," *IEEE Commun. Mag.*, vol. 56, no. 9, pp. 162–169, Sep. 2018.

[23] W. Saad, M. Bennis, and M. Chen, "A vision of 6G wireless systems: Applications, trends, technologies, and open research problems," *IEEE Netw.*, vol. 34, no. 3, pp. 134–142, May/Jun. 2020.

[24] Y. Rong, X. Tang, and Y. Hua, "A unified framework for optimizing linear nonregenerative multicarrier MIMO relay communication systems," *IEEE Trans. Signal Process.*, vol. 57, no. 12, pp. 4837–4851, Dec. 2009.

[25] Z. Ding, I. Krikidis, B. Rong, J. S. Thompson, C. Wang, and S. Yang, "On combating the half-duplex constraint in modern cooperative networks: Protocols and techniques," *IEEE Wireless Commun.*, vol. 19, no. 6, pp. 20–27, Dec. 2012.

[26] H. Li, Q. Liu, Z. Wang, and M. Li, "Joint antenna selection and analog precoder design with low-resolution phase shifters," *IEEE Trans. Veh. Technol.*, vol. 68, no. 1, pp. 967–971, Jan. 2019.

[27] L.-H. Gao *et al.*, "Broadband diffusion of terahertz waves by multi-bit coding metasurfaces," *Light, Sci. Appl.*, vol. 4, no. 9, Sep. 2015, Art. no. e324.
[28] D. Mishra and H. Johansson, "Channel estimation and low-complexity beamforming design for passive intelligent surface assisted MISO wireless energy transfer," in *Proc. IEEE Int. Conf. Acoust., Speech Signal Process. (ICASSP)*, Brighton, U.K., May 2019, pp. 4659–4663.
[29] Z.-Q. He and X. Yuan, "Cascaded channel estimation for large intelligent metasurface assisted massive MIMO," *IEEE Wireless Commun. Lett.*, vol. 9, no. 2, pp. 210–214, Feb. 2020.
[30] W. Yan, X. Yuan, and X. Kuai, "Passive beamforming and information transfer via large intelligent surface," *IEEE Wireless Commun. Lett.*, vol. 9, no. 4, pp. 533–537, Apr. 2020.
[31] Q.-U.-A. Nadeem, A. Kammoun, A. Chaaban, M. Debbah, and M.-S. Alouini, "Asymptotic max-min SINR analysis of reconfigurable intelligent surface assisted MISO systems," *IEEE Trans. Wireless Commun.*, vol. 19, no. 12, pp. 7748–7764, Dec. 2020.
[32] Y. Shuang, H. Zhao, H. Li, M. Wei, and L. Li, "Dynamic energy allocation of commondity Wi-Fi signals using programmable coding metasurface," in *Proc. Int. Appl. Comput. Electromagn. Soc. Symp. China (ACES)*, Aug. 2019, pp. 1–2.
[33] Y. Liu, L. Zhang, P. V. Klaine, and M. A. Imran, "Optimal multi-user transmission based on a single intelligent reflecting surface," in *Proc. IEEE 4th Int. Conf. Electron. Inf. Commun. Technol. (ICEICT)*, Aug. 2021, pp. 1–4.
[34] W. Tang *et al.*, "Wireless communications with reconfigurable intelligent surface: Path loss modeling and experimental measurement," 2019, *arXiv:1911.05326*.
[35] P. Cao, J. S. Thompson, and H. Haas, "Constant modulus shaped beam synthesis via convex relaxation," *IEEE Antennas Wireless Propag. Lett.*, vol. 16, pp. 617–620, 2017.
[36] X. Gao, L. Dai, S. Han, I. Chih-Lin, and R. W. Heath, "Energy-efficient hybrid analog and digital precoding for mmWave MIMO systems with large antenna arrays," *IEEE J. Sel. Areas Commun.*, vol. 34, no. 4, pp. 998–1009, Apr. 2016.
[37] F. Sohrabi and W. Yu, "Hybrid analog and digital beamforming for mmWave OFDM large-scale antenna arrays," *IEEE J. Sel. Areas Commun.*, vol. 35, no. 7, pp. 1432–1443, Jul. 2017.
[38] Q. Wu and R. Zhang, "Towards smart and reconfigurable environment: Intelligent reflecting surface aided wireless network," *IEEE Commun. Mag.*, vol. 58, no. 1, pp. 106–112, Jan. 2020.
[39] D. Mishra and E. G. Larsson, "Passive intelligent surface assisted MIMO powered sustainable IoT," in *Proc. IEEE Int. Conf. Acoust., Speech Signal Process. (ICASSP)*, May 2020, pp. 8961–8965.
[40] Q.-U.-A. Nadeem, H. Alwazani, A. Kammoun, A. Chaaban, M. Debbah, and M.-S. Alouini, "Intelligent reflecting surface-assisted multi-user MISO communication: Channel estimation and beamforming design," *IEEE Open J. Commun. Soc.*, vol. 1, pp. 661–680, 2020.
[41] S. Guo, S. Lv, H. Zhang, J. Ye, and P. Zhang, "Reflecting modulation," *IEEE J. Sel. Areas Commun.*, vol. 38, no. 11, pp. 2548–2561, Nov. 2020.
[42] Z. Wang, L. Liu, and S. Cui, "Channel estimation for intelligent reflecting surface assisted multiuser communications: Framework, algorithms, and analysis," *IEEE Trans. Wireless Commun.*, vol. 19, no. 10, pp. 6607–6620, Oct. 2020.
[43] E. Björnson, "Optimizing a binary intelligent reflecting surface for OFDM communications under mutual coupling," 2021, *arXiv:2106.04280*.
[44] L. Zhang and W. Liu, "Robust beamforming for coherent signals based on the spatial-smoothing technique," *Signal Process.*, vol. 92, no. 11, pp. 2747–2758, Nov. 2012.
[45] L. Zhang, W. Liu, and R. J. Langley, "A class of constrained adaptive beamforming algorithms based on uniform linear arrays," *IEEE Trans. Signal Process.*, vol. 58, no. 7, pp. 3916–3922, Jul. 2010.
[46] P. T. Boggs and W. J. Tolle, "Sequential quadratic programming for large-scale nonlinear optimization," *J. Comput. Appl. Math.*, vol. 124, nos. 1–2, pp. 123–137, 2000. [Online]. Available: http://www.sciencedirect.com/science/article/pii/S0377042700004295
[47] A. Hessel, J. Schmoys, and D. Y. Tseng, "Bragg-angle blazing of diffraction gratings," *J. Opt. Soc. Amer.*, vol. 65, no. 4, p. 380, 1975.
[48] H. Guo, B. Makki, and T. Svensson, "A genetic algorithm-based beamforming approach for delay-constrained networks," in *Proc. 15th Int. Symp. Modeling Optim. Mobile, Ad Hoc, Wireless Netw. (WiOpt)*, May 2017, pp. 1–7.

Yihong Liu (Graduate Student Member, IEEE) received the B.Eng. degree (Hons.) in electronics and electrical engineering from the Glasgow College, University of Electronic Science and Technology of China (UESTC), Chengdu, Sichuan, China, in 2018. He is currently pursuing the Ph.D. degree with the James Watt School of Engineering, University of Glasgow. His current research interests include signal processing for wireless communications, with a focus on MIMO systems, array signal processing, intelligent reflecting surfaces, and physical layer security. He has received the IEEE ICEICT'21 Best Paper Award.

Lei Zhang (Senior Member, IEEE) is currently a Senior Lecturer at the University of Glasgow. He has academia and industry combined research experience on wireless communications and networks and distributed systems for the IoT, blockchain, and autonomous systems. His 20 patents are granted/filed in more than 30 countries/regions. He has published three books, more than 150 papers in peer-reviewed journals and conferences, and edited books. He has received the IEEE ComSoc TAOS Technical Committee Best Paper Award 2019 and the IEEE ICEICT'21 Best Paper Award. He is the Founding Chair of IEEE Special Interest Group on Wireless Blockchain Networks in Cognitive Networks Technical Committee (TCCN). He has delivered tutorials in IEEE ICC'20, IEEE PIMRC'20, IEEE GLOBECOM'21, IEEE VTC'21 Fall, IEEE ICBC'21, and EUSIPCO'21. He is an Associate Editor of IEEE INTERNET OF THINGS JOURNAL, IEEE WIRELESS COMMUNICATIONS LETTERS, and *Digital Communications and Networks*. He is a Guest Editor of IEEE JOURNAL ON SELECTED AREAS IN COMMUNICATIONS.

Muhammad Ali Imran (Senior Member, IEEE) is currently the Dean of UESTC, University of Glasgow. He is also a Professor of wireless communication systems with research interests in fundamental communication theory, self-organized networks, and the wireless sensor systems. He heads the Communications, Sensing and Imaging (CSI) Research Group, University of Glasgow; and the Director of the Centre for Educational Development and Innovation. He is an Affiliate Professor at The University of Oklahoma, USA; an Adjunct Research Professor at Ajman University, United Arab Emirates; and a Visiting Professor at the 5G Innovation Centre, University of Surrey, U.K. He has over 20 years of combined academic and industry experience with several leading roles in multi-million pounds funded projects. He has filed 15 patents. He has authored/coauthored over 400 journals and conference publications. He has authored two books, edited eight books, and authored more than 30 book chapters. He has successfully supervised over 40 postgraduate students at doctoral level. He has been a consultant to international projects and local companies in the area of self-organized networks. He is a fellow of IET and a Senior Fellow of HEA.